Universitat Politécnica de Catalunya

and

Barcelona Supercomputing Center

Internship Report

A Study on Different Parameterizations for 1D Helmholtz Equation with Proper Generalized Decomposition

---

Author:

ANQI LI

Supervised by
Dr. David Modesto
Barcelona Supercomputing Center

Supervised by
Prof. Sergio Zlotnik
Universitat Politécnica de Catalunya

Barcelona, June 27, 2017

Contents

List of Figures

1 Introduction

The identification of subsoil structures and layers beneath the ocean, especially the physical properties and dimensions is a very important task in geophysics. It has numerous application, for example discovering oil, natural gas or minerals. The common method is using a seismic source to generates controlled seismic waves that travel through a medium such as water or layers of rocks. Some of the waves will reflect and refract and are recored at receivers. The data collected can then be used to investigate shallow subsoil structure or in search for petroleum and mineral deposits, or to map subsurface faults.

The propagation of the wave induced by a seismic source can be modeled in terms of Helmholtz equation with point source. Also, the problem depends highly on the parameters (e.g. frequency and velocity, etc.) to describe specific geometric or material properties of the subsoil. For specified parameters, the problem can be solved by standard discretization techniques(e.g. FEM). However, in engineering practice, such computation is required to be carried out repeatedly with different values of parameter for an identification analysis or an optimization strategy. Such computations are costly and inefficient.

Therefore, a strategy is needed to reduce the computation costs by allowing to solve a number of Helmholtz equation for different choices of the parameters in an efficient way. The idea is to construct the generalized (parameterized) Helmholtz equation by including the parameters (such as velocity and frequency) as a variable in the differential equation. However, the high-dimensional problem composed by including parameters as extra dimensions involves an exponential growth of degrees of freedom, see [1, 2, 3, 4, 5]. In order to lower the computational complexity, reduce the degrees of the problem, the model that is based on an approximation to the original model is called Reduced Order Model (ROM). By doing this, the reduced-order model can then be evaluated in significantly less time with a bit compromising on accuracy.(Examples of ROM methods are, for example, the Proper Orthogonal Decomposition (POD) method [6, 7, 8, 9] or the Reduced Basis method [4, 5, 10, 11])

Among all the ROM methods, the Proper Generalized Decomposition (PGD)[12, 13] method is used in this report. It has been studied and successfully applied to various problems in computational mechanics, see [14, 15, 16, 17, 18] There are two phrases for using PGD: the off-line phrase where all the separated approximations are computed and is costly as always, and an on-line phase where the specific solution at any desired parameter is readily obtained by means of fast post-process. In this way, the on-line phase does not require solving any more differential problem and the PGD approximation can be accessed in real-time. Only standard PGD is apply in the report, [19, 20, 21] addressed different PGD techniques.

In order to reduce the complicity, only 1D domain is tested in the report. Also, as there are several possibilities to parameterize the problem, here we only focus on the angular frequency and the velocity of the wave. For practical application, besides one uniform velocity among the domain, multiple values of velocity can be assigned to different part of the domain.

This report is organized as following.

The next chapter we present briefly introduce the Helmholtz equation and the Proper generalized decomposition (PGD) method. And on the base of that, the formulation for multiple layers of velocity. The third chapter presents the numerical application of the PGD method, among which 4 cases is discussed. The first case is to parametrize only frequency with the spatial domain and analyze three different types of parametrization for frequency. The second case is similar to the first case but for the velocity. The third case is to combine both frequency and velocity with the spatial domain, using the optimal parametrization choice for the two parameters discussed in the previous case. The last case will be testing the behavior of the method considering two layers of velocity in the spatial domain.

2 Numerical Methodology

2.1 Generalized Helmholtz Equation

The Helmholtz Equation for a 1D domain that governs the problem takes the form,

$$\Delta u + k^2 u = f \quad in \quad \Omega_\infty \tag{2.1}$$

where Δ is the Laplacian, $k(x) \in \mathbb{R}$ is the angular wavenumber, u is the displacement field, and f is the source term. The angular wavenumber ω is related frequency w and the velocity v and wavelength λ,

$$k = \frac{\omega}{v}, \quad k = 2\pi\lambda$$

The Dirichlet boundary condition is defined on the boundary of the domain (two points on the two sides of the 1D domain).

$$u = 0 \quad in \ \Gamma_D$$

The solution of Eq.2.1 can be obtained by using standard discretization techniques, for a desired frequency, velocity and source.

The generalized (parametrized) Helmholtz Equation can be formalized for any frequency ω and velocity v by accounting the parameters as extra dimensions of the problem based on the strong form in Eq.2.1. The displacement field can then be written as $u(x, \omega, v)$ which is a function of spatial coordinates $x \in \Omega$, angular frequency $\omega \in I_\omega$ and velocity $v \in I_v$. To obtain the weak form for the generalized Helmholtz Equation, multiply weighting function δu on both side and integrate along the spatial, frequency and velocity domain,

$$\int_{\Omega \times I_\omega \times I_v} (\Delta u + k^2 u)\delta u \ dx d\omega dv = \int_{\Omega \times I_\omega \times I_v} f \delta u \ dx d\omega dv \tag{2.2}$$

Apply integration by parts and the generalized Helmholtz Equation can be obtained as,

$$-(\nabla u, \nabla \delta u)_{\Omega \times I_\omega \times I_v} + (k^2 u, \delta u)_{\Omega \times I_\omega \times I_v} = (f, \delta u)_{\Omega \times I_\omega \times I_v} \tag{2.3}$$

for all δu in the proper selected space.

2.2 Proper generalized decomposition (PGD)

The reduced order method introduced here approximates the generalized solution of Eq.2.3 by assuming that the solution can be written in separable form as,

$$u(x, \omega, v) \approx u^n(x, \omega, v) = \sum_{m=1}^{n} F_1^m(x) F_2^m(\omega) F_3^m(v) \tag{2.4}$$

This approach will have to determine the number of necessary modes n, see [24] and the unknown function F_1^m, $F_2^m$and F_3^m for $m = 1, ..., n$. Each mode m can be obtained by a greedy algorithm, that is

$$u(x, \omega, v) = u^{n-1}(x, \omega, v) + F_1(x)F_2(\omega)F_3(v) \tag{2.5}$$

where u^{n-1} is assumed to be already known, F_1, F_2 and F_3 are the only functions of the unknown term. By replacing Eq.2.5 in Eq.2.3, the problem to be solved now becomes,

$$\begin{aligned} -(F_2(\omega)F_3(v)\nabla F_1(x), \nabla \delta u)_{\Omega \times I_\omega \times I_v} + (k^2 F_1(x)F_2(\omega)F_3(v), \delta u)_{\Omega \times I_\omega \times I_v} = \\ (f, \delta u)_{\Omega \times I_\omega \times I_v} - [-(\nabla u^{n-1}, \nabla \delta u)_{\Omega \times I_\omega \times I_v} + (k^2 u^{n-1}, \delta u)_{\Omega \times I_\omega \times I_v}] \end{aligned} \tag{2.6}$$

This is a nonlinear problem with the three unknowns F_1 F_2 and F_3. In order to solve the above equation, assume the weighted function δu can be expresses in separable form as,

$$\delta u = \delta F_1(x)F_2(\omega)F_3(v) + F_1(x)\delta F_2(\omega)F_3(v) + F_1(x) \ F_2(\omega)\delta F_3(v) \tag{2.7}$$

Eq.2.6 defines the nonlinear equation to be solved for the generalized solution. Using 2.7, the nonlinear problem (2.6) can be solved with a linearized scheme, see [20, 21] and iterate until a proxy for termination is reached.

2.2.1 Standard PGD

The fixed point iteration proceed the following three steps:

1 Assume that F_2 and F_3 are known($\delta F_2 = 0$, $\delta F_3 = 0$). And Eq.2.7 can then be written as,

$$\delta u = \delta F_1 F_2 F_3 \tag{2.8}$$

And the problem to be solved becomes

$$\begin{aligned} -(F_2F_3\nabla F_1, \nabla \delta F_1 F_2 F_3)_{\Omega\times I_\omega \times I_v} + (k^2 F_1F_2F_3, \delta F_1F_2F_3)_{\Omega\times I_\omega\times I_v} = (f, \delta F_1F_2F_3)_{\Omega\times I_\omega\times I_v} \\ - [-(\nabla u^{n-1}, \nabla \delta F_1F_2F_3)_{\Omega\times I_\omega\times I_v} + (k^2u^{n-1}, \delta F_1F_2F_3)_{\Omega\times I_\omega\times I_v}] \end{aligned} \tag{2.9}$$

for all δF_1

2 Assume that F_1 is known from the previous step ($\delta F_1 = 0$) and F_3 is known ($\delta F_3 = 0$). And Eq.2.7 can then be written as,

$$\delta u = F_1 \delta F_2 F_3 \tag{2.10}$$

And the problem to be solved becomes

$$\begin{aligned} -(F_2F_3\nabla F_1, \nabla F_1 \delta F_2 F_3)_{\Omega\times I_\omega \times I_v} + (k^2 F_1F_2F_3, F_1\delta F_2F_3)_{\Omega\times I_\omega\times I_v} = (f, F_1\delta F_2F_3)_{\Omega\times I_\omega\times I_v} \\ - [-(\nabla u^{n-1}, \nabla F_1\delta F_2F_3)_{\Omega\times I_\omega\times I_v} + (k^2u^{n-1}, F_1\delta F_2F_3)_{\Omega\times I_\omega\times I_v}] \end{aligned} \tag{2.11}$$

for all δF_2

3 Assume that F_1 and F_2 are known from the previous step ($\delta F_1 = 0$, $\delta F_2 = 0$) . And Eq.2.7 can then be written as,

$$\delta u = F_1 F_2 \delta F_3 \tag{2.12}$$

And the problem to be solved becomes

$$\begin{aligned} -(F_2F_3\nabla F_1, \nabla F_1 F_2 \delta F_3)_{\Omega\times I_\omega \times I_v} + (k^2 F_1F_2F_3, F_1F_2\delta F_3)_{\Omega\times I_\omega\times I_v} = (f, F_1F_2\delta F_3)_{\Omega\times I_\omega\times I_v} \\ - [-(\nabla u^{n-1}, \nabla F_1F_2\delta F_3)_{\Omega\times I_\omega\times I_v} + (k^2u^{n-1}, F_1F_2\delta F_3)_{\Omega\times I_\omega\times I_v}] \end{aligned} \tag{2.13}$$

for all δF_3

This iterative algorithm is required for each step of the greedy procedure. Note that an original 3D problem is now reduced to the iteration of one 1D problem (Eq.2.9) and two 1D algebraic equations (Eq. 2.11 and 2.13). As the second and third step is an algebraic equations, no derivatives with respect to the parameters exist in the strong form of the Helmholtz equation (2.1), the computational costs of step two and three can be ignored. Therefore, the computational cost of the PGD approximation is the product of the cost of 1D solve, the number of iterations performed and the number of terms required to reach the desired accuracy.

2.2.2 Convergence criteria

The PGD reduced order method requires a criteria for the termination for PGD approximation terms in Eq.2.5 and for the fixed point algorithm in Eq.2.9, Eq.2.11 and Eq.2.13, see [25]. In order to terminate the PGD approximation when enough terms are generated, it is evaluated by comparing the contribution of the last term against the products of all the previous terms,

$$\frac{\|F_1F_2F_3\|^2}{\|u^{n-1}\|^2_{\mathcal{L}2}} < \epsilon^2 \tag{2.14}$$

Also, the fixed point algorithm converges when the following relationship is fulfilled,

$$\frac{\|F_1^{(\nu)}F_2^{(\nu)}F_3^{(\nu)} - F_1^{(\nu-1)}F_2^{(\nu-1)}F_3^{(\nu-1)}\|^2_{\mathcal{L}2}}{\|F_1^{(\nu)}F_2^{(\nu)}F_3^{(\nu)}\|^2_{\mathcal{L}2}} < \epsilon^2 \tag{2.15}$$

where ν is the iteration counter. The maximum number of iteration is imposed in case that the algorithms can not converge.

2.3 Multiple layers of velocity

Due to the practical needs, more than one velocity will be assigned to the domain. Separate the domain into p sub-domains Ω_p and ascribe each with a velocity. For simplify the expressions, this section will produce the velocity in terms of the following notation, $u(x, \frac{1}{v_1^2}, \frac{1}{v_2^2}, ..., \frac{1}{v_p^2}) \equiv u(x, \hat{v}_1, \hat{v}_2, ..., \hat{v}_p)$. The velocity profile of the problem can then be written as,

$$\hat{v}(x) = \sum_{i=1}^{p} \varphi_i(x)\hat{v}_i \tag{2.16}$$

where $\varphi_i(x)$ is the wighted function, and is simply defines as,

$$\varphi_i(x) = \begin{cases} 1, & \text{when } x \in \Omega_i \\ 0, & \text{adhersive} \end{cases}$$

In order to simplify the derivation, consider that the generalized solution depends on spatial coordinates and the velocities in each sub-domains. Then the PGD expression (2.4) can be expressed as,

$$u(x, \hat{v}_1, ..., \hat{v}_p) \approx u^n(x, \hat{v}_1, ..., \hat{v}_p) = \sum_{m=1}^{n} F_1^m(x) \prod_{i=2}^{p+1} F_i^m(\hat{v}_i) \tag{2.17}$$

For demonstration, assume two sub-domains (Ω_1 and Ω_2), the velocity profile then becomes,

$$\hat{v}(x) = \varphi_1(x)\hat{v}_1 + \varphi_2(x)\hat{v}_2 \tag{2.18}$$

And the greedy algorithm (2.5) can be written as,

$$u(x, v_1, v_2) = u^{n-1}(x, v_1, v_2) + F_1(x)F_2(v_1)F_3(v_2) \tag{2.19}$$

The iteration algorithm introduced above then becomes,

1 Assume that F_2 and F_3 are known ($\delta F_2 = 0$, $\delta F_3 = 0$).

$$\delta u = \delta F_1 F_2 F_3$$

And the problem to be solved become

$$\begin{aligned} &-(F_2F_3\nabla F_1, \nabla \delta F_1 F_2 F_3)_{\Omega \times I_{v_1} \times I_{v_2}} \\ &\quad +\omega^2 \Big[(\varphi_1 F_1, \delta F_1)_\Omega (\hat{v}_1 F_2, F_2)_{I_{v_1}} (F_3, F_3)_{I_{v_2}} + (\varphi_2 F_1, \delta F_1)_\Omega (F_2, F_2)_{I_{v_1}} (\hat{v}_2 F_3, F_3)_{I_{v_2}} \Big] \\ &\qquad = (f, \delta F_1 F_2 F_3)_{\Omega \times I_{v_1} \times I_{v_2}} - \Big[-(\nabla u^{n-1}, \nabla \delta F_1 F_2 F_3)_{\Omega \times I_{v_1} \times I_{v_2}} \\ &\qquad\qquad + \omega^2 \Big((\varphi_1 \hat{v}_1 + \varphi_2 \hat{v}_2) u^{n-1}, \delta F_1 F_2 F_3 \Big)_{\Omega \times I_{v_1} \times I_{v_2}} \Big] \end{aligned} \tag{2.20}$$

for all δF_1

2 Assume that F_1 is known from the previous step ($\delta F_1 = 0$) and F_3 is known ($\delta F_3 = 0$).

$$\delta u = F_1 \delta F_2 F_3$$

And the problem to be solved become

$$\begin{aligned} &-(F_2F_3\nabla F_1, \nabla F_1 \delta F_2 F_3)_{\Omega \times I_{v_1} \times I_{v_2}} \\ &\quad +\omega^2 \Big[(\varphi_1 F_1, F_1)_\Omega (\hat{v}_1 F_2, \delta F_2)_{I_{v_1}} (F_3, F_3)_{I_{v_2}} + (\varphi_2 F_1, F_1)_\Omega (F_2, \delta F_2)_{I_{v_1}} (\hat{v}_2 F_3, F_3)_{I_{v_2}} \Big] \\ &\qquad = (f, F_1 \delta F_2 F_3)_{\Omega \times I_{v_1} \times I_{v_2}} - \Big[-(\nabla u^{n-1}, \nabla F_1 \delta F_2 F_3)_{\Omega \times I_{v_1} \times I_{v_2}} \\ &\qquad\qquad + \omega^2 \Big((\varphi_1 \hat{v}_1 + \varphi_2 \hat{v}_2) u^{n-1}, F_1 \delta F_2 F_3 \Big)_{\Omega \times I_{v_1} \times I_{v_2}} \Big] \end{aligned} \tag{2.21}$$

for all δF_2

3 Assume that F_1 and F_2 are known from the previous step ($\delta F_1 = 0$, $\delta F_2 = 0$).

$$\delta u = F_1 F_2 \delta F_3$$

And the problem to be solved become

$$\begin{aligned} &-(F_2F_3\nabla F_1, \nabla F_1F_2\delta F_3)_{\Omega\times I_{v_1}\times I_{v_2}} \\ &\quad +\omega^2\Big[(\varphi_1F_1, F_1)_\Omega(\hat{v}_1F_2, F_2)_{I_{v_1}}(F_3, \delta F_3)_{I_{v_2}} + (\varphi_2F_1, F_1)_\Omega(F_2, F_2)_{I_{v_1}}(\hat{v}_2F_3, \delta F_3)_{I_{v_2}}\Big] \\ &\qquad = (f, F_1F_2\delta F_3)_{\Omega\times I_{v_1}\times I_{v_2}} - \Big[-(\nabla u^{n-1}, \nabla F_1F_2\delta F_3)_{\Omega\times I_{v_1}\times I_{v_2}} \\ &\qquad\qquad +\omega^2\Big((\varphi_1\hat{v}_1 + \varphi_2\hat{v}_2)u^{n-1}, F_1F_2\delta F_3\Big)_{\Omega\times I_{v_1}\times I_{v_2}}\Big] \end{aligned} \tag{2.22}$$

for all δF_3.

3 Numerical application

The Model is based on the Eq.2.1, and the 1D domain is set specifically as $[0, 1]$ with point source located at $x = 0.5$. Without further notice, the range of the parameter dimensions are interpreted by setting the maximum and minimum wavenumber λ inside the domain, 10 and 1 respectively. As the wavenumber only indicates the relationship between velocity and frequency, for testing on frequency, velocity is fixed to be 0.1 which gives the range of frequency to be $\omega \in [0.6283, 6.2832]$. Similarly, for testing on velocity, frequency is set as 10 and the corresponding velocity range is $v \in [0.1592, 1.5915]$.

The minimum wave resolution in the spatial domain is 15 nodes. For the parameter domain, the number of nodes is designed as 5000. Furthermore, the tolerance for the last PGD term (2.14) is 10^{-16} and for the fixed point algorithm (2.15) is 10^{-6}, exceptions will be specify in the case.

3.1 Case 1: Variable frequency

For frequency ω, three types of parametric representations are tested, w, k and k^2 respectively. In the interests of finding the best parametrization for frequency, Figure 3.1 plots the PGD error of $u(x, \omega)$, $u(x, k)$ and $u(x, k^2)$for all frequencies. It can be observed from Figure 3.1 that for three types of parametrization, the PGD errors have the similar behavior, for certain frequencies all the parameterizations are not behaving well, most likely is due to the resonance effect as the domain is defined to be a interior (or closed) domain. The location of the maximum PGD error for each parametrization is marked by the green dot in Figure 3.1. Meanwhile, Figure 3.3 plot the displacement field from both FEM and PGD for the certain frequency where the maximum PGD error occurred for the corresponding parametrization. From Figure 3.3, it can be detected that the PGD methods have the same phase as the FEM solution, but can not capture the wave height.

Figure 3.2 plot the PGD error indicator against number of modes, all three parametrization converged in the end. However, $u(x, k^2)$ take significant more number of modes (144 modes) than $u(x, \omega)$ (60 modes) and $u(x, k)$ (49 modes). By comparing both Figure 3.2 and 3.1, the best parametrization for frequency should be $u(x, \omega)$ and $u(x, k)$, among which $u(x, \omega)$ have better performance in low frequency (roughly from 0.6 to 3) while $u(x, k)$ is better in high frequency (from 4 to 6.3).

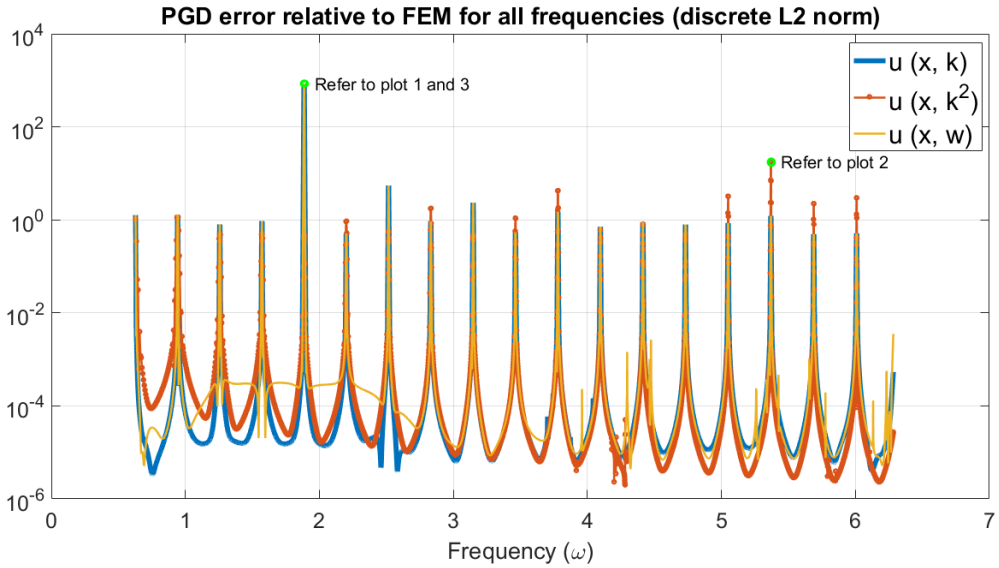

Figure 3.1: PGD error for all frequencies

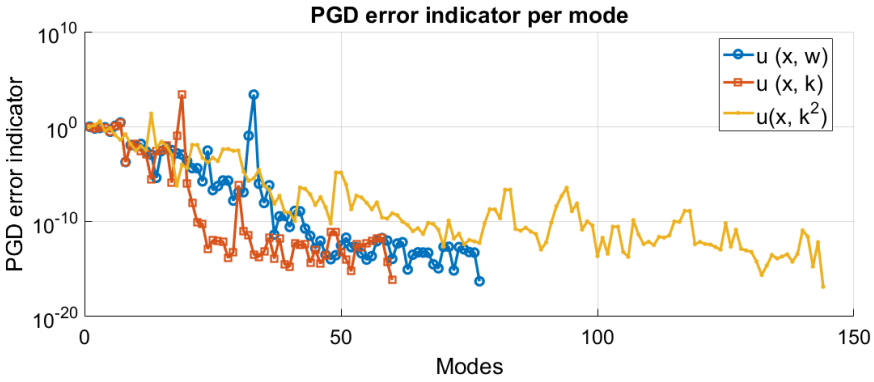

Figure 3.2: PGD error indicator for each modes

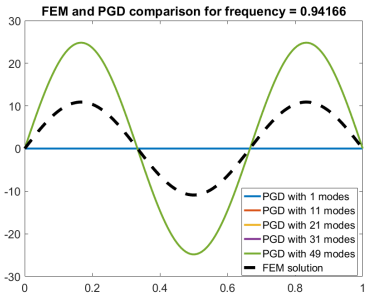

(a) Plot 1: The displacement field by PGD and FEM solution for the parametrization $u(x, w)$ with the maximum PGD error

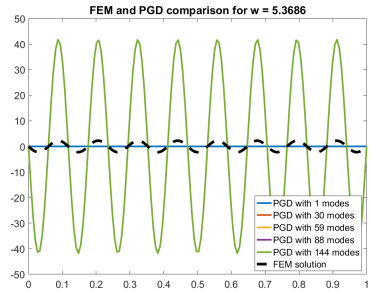

(b) Plot 2: the displacement field by PGD and FEM solution for the parametrization $u(x, k^2)$ with the maximum PGD error

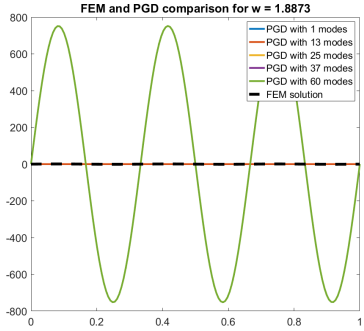

(c) Plot 3: the displacement field by PGD and FEM solution for the parametrization $u(x, k)$ with the maximum PGD error

Figure 3.3: The displacement field by PGD and FEM solution for the frequency parameterizations

3.2 Case 2: Variable velocity

The parametrizations for velocity are v, $1/v$, $1/v^2$ respectively. The similar analyses for frequency are carried out here. Figure 3.4 presents the PGD error of velocity parameterizations for all velocities. And in order to observe better, Figure 3.5 zoomed in the right side of the Figure 3.4.

Similar as Figure 3.1, there are certain values of velocity that all parameterization is not performing well. However, it is obvious that different parametrization have its own favored region. For low velocity values, which indicates a high frequency and shorter waves, the parametrization using inverse of the velocity has smaller error, i.e. $u(x, 1/v^2)$. For high velocity values, which indicates a low frequency and long wave length, the parametrization using $u(x, v)$ has better behavior. Figure 3.6 plot the PGD error indicator

against the number of modes. All parametrization is able to converge in the end, 195 modes for $u(x, v)$, 165 for $u(x, 1/v)$and 188 for $u(x, 1/v^2)$.

Figure 3.7 plotted four figures regarding the parametrization $u(x, 1/v^2)$ and $u(x, v)$ respectively each for minimum and maximum PGD error. The location of the plot is also marked by green dot in Figure 3.4 and 3.5. The same conclusions can be draw from Figure 3.7c and Figure 3.7a that the PGD methods can capture the phrase of the FEM solution, but not the wave height. Among all 3 parametrization, $u(x, 1/v)$ is the least favorite, for high velocity $u(x, 1/v^2)$ is preferable and for low velocity $u(x, v)$ is better.

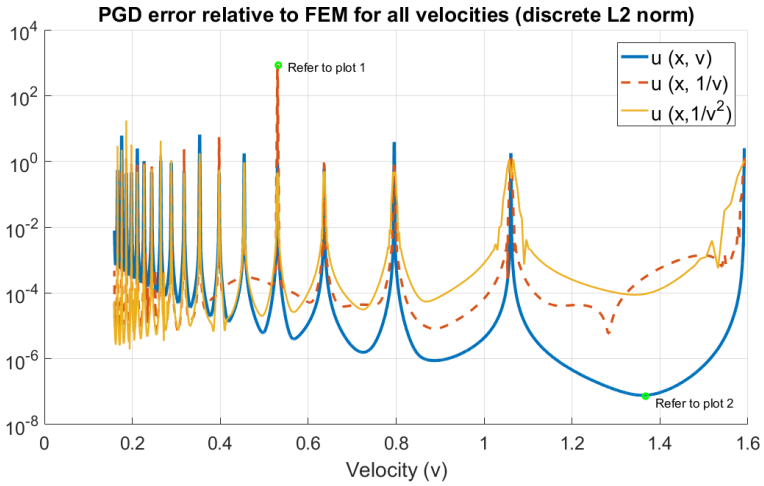

Figure 3.4: PGD error for all velocities

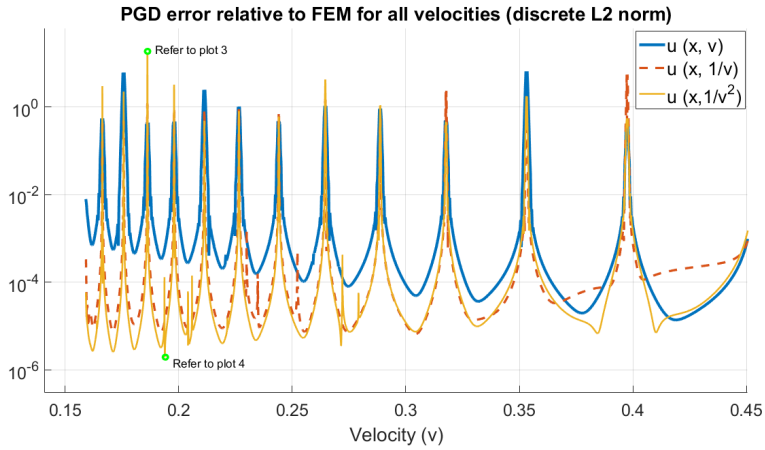

Figure 3.5: PGD error for all velocities (zoom-in right side of the Figure 3.4)

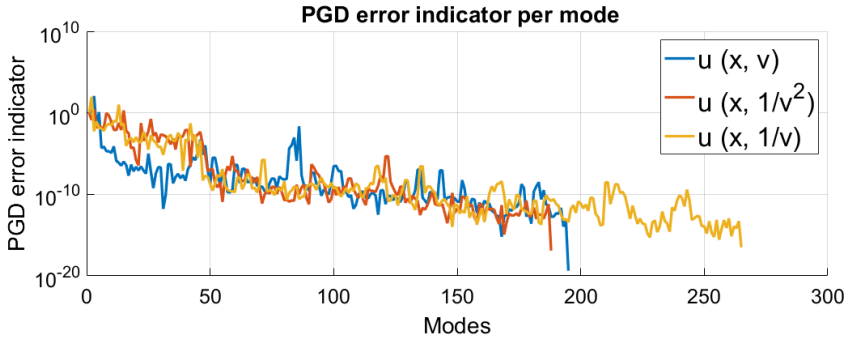

Figure 3.6: PGD error indicators for each mode

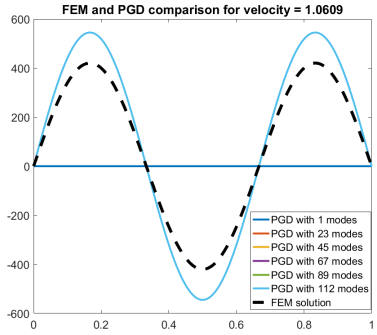

(a) Plot 1: For $u(x, v)$, the PGD and FEM displacement field for maximum PGD error ($error = 1.7887$)

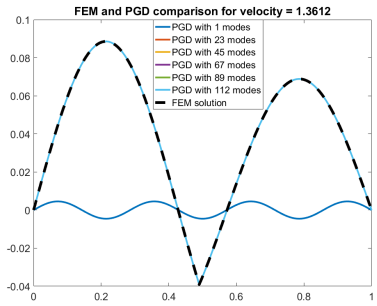

(b) Plot 2: For $u(x, v)$, the PGD and FEM displacement field for minimum PGD error ($error = 7.7429 \times 10^{-8}$)

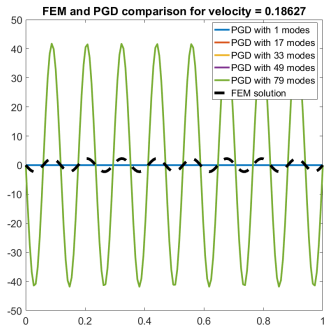

(c) Plot 3: For $u(x, 1/v^2)$, the PGD and FEM displacement field for maximum PGD error ($error = 17.4064$)

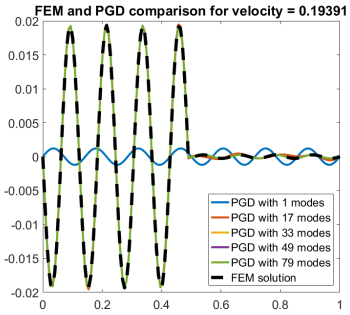

(d) Plot 4: For $u(x, 1/v^2)$, the PGD and FEM displacement field for minimum PGD error ($error = 1.9195 \times 10^{-6}$)

Figure 3.7: The displacement field by PGD and FEM solution for the velocity parameterizations

3.3 Case 3: Variable frequency and velocity

In this case, combine both velocity and frequency with the spatial domain. The parameter domain of velocity and frequency will use the ones that is tests above, $\omega \in [0.6283, 6.2832]$ and $v \in [0.1592, 1.5915]$, which gives a wavenumber $k \in [0.3948, 39.4784]$. Taking as a reference the results obtained in case 1 and case 2, the generalized solution of is parametrized in terms of $u(x, \omega, \frac{1}{v^2})$. From Figure 3.8 and 3.9, it is clear the the standard PGD failed to obtained the correct solution. Figure 3.8 plot the PGD error with respect to FEM against both frequency and velocity, the error is around 1 which indicates 100% error. In Figure 3.9 with 500 modes the method cannot converge.

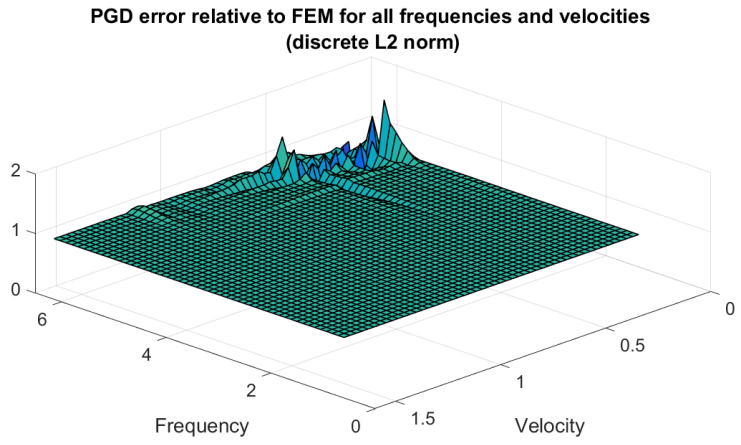

Figure 3.8: PGD errors for all velocities and frequencies

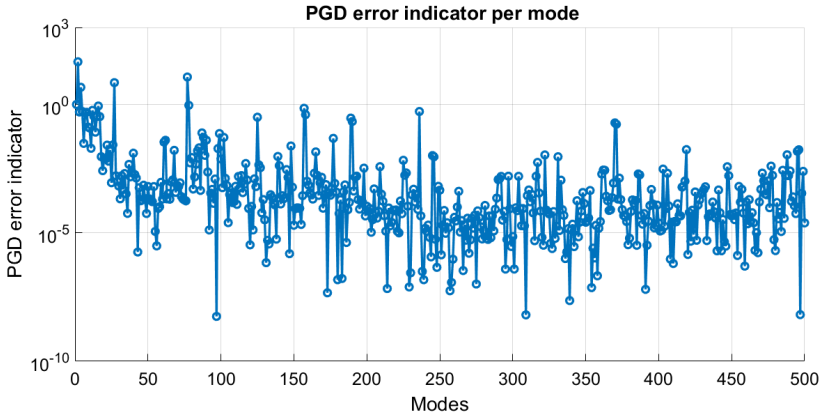

Figure 3.9: PGD error indicators for each mode

To validate the method, we reduce the range of the wavenumber in order to apply a smaller range of parameter domain to run the simulation again. Figure 3.10 and 3.11 is the results obtained by using wavenumber $\lambda \in [1, 2]$, which correspondingly gives the frequency between 0.6283 and 1.2566, and the velocity between 1.5915 and 0.7958. The error in 3.10 is oscillating from both parameter dimensions (frequency and velocity) but with a fairly small magnitude (under 10^{-7}) which proves that the PGD solution is close to the FEM.

The above two examples indicate that to parametrize both frequency and velocity with standard PGD, the method can obtained the correct results, comparing with FEM, only for small parameter range (or say wave number), but not for large range. As discussed before, there are certain frequency and velocity that the PGD method have trouble with (referring to 3.2 and 3.4), and when combing both frequency and velocity the standard PGD method will have trouble obtaining the reasonable solution for large range as more of those points is introduced in. In order to solve this problem, one way of solving it is to parametrize the displacement field in terms of $u(x, k)$,as presented in the following case (Case 4), where k includes the varying in both velocity and frequency or using improved PGD method, such as Petrov-Galerkin PGD (PG PGD).[20]

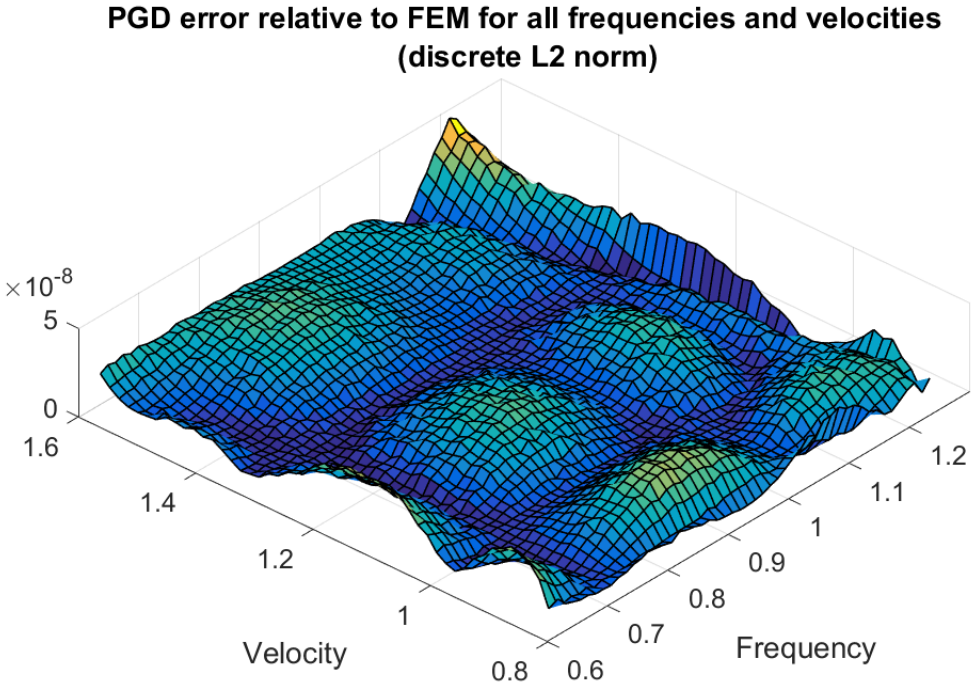

Figure 3.10: PGD errors for all velocities and frequencies

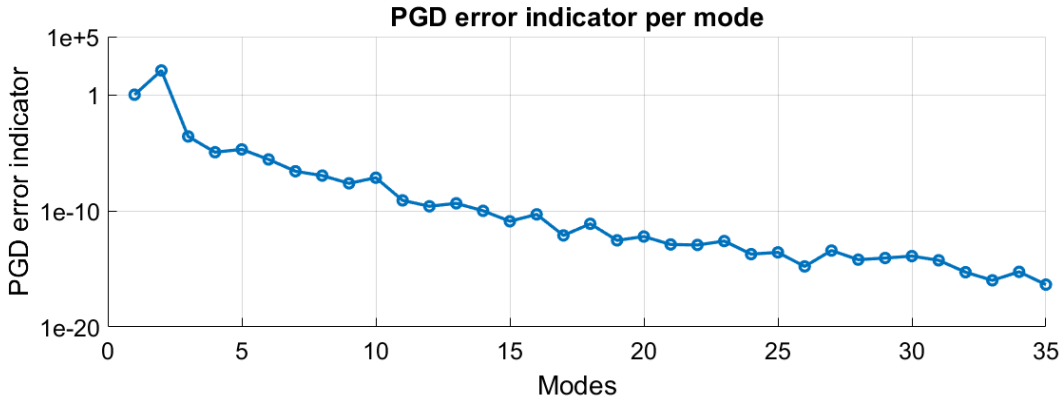

Figure 3.11: PGD error indicators for each mode

3.4 Case 4: Variable wavenumber

As explained in the previous case, in order to prevent the problem by parametrize the generalized solution in terms of $u(x, \omega, 1/v^2)$, parametrize the solution as $u(x, k)$ as the varying of frequency and velocity influence only the angular wavenumber k. The range for the wavenumber between 1 and 10 waves is given in the previous case, $k \in [0.3948, 39.4784]$. Need to mention, this case does look similar as Case 1 since the parametrization is the same. However, in this case as the velocity is varying as well so the wavenumber domain I_k differs from Case 1.

The PGD error with respect to the FEM solution (Figure 3.12) is similar as Figure 3.2, as there are still exists of some wavenumber that the method has problem with. From Figure 3.13 it can observe that the convergence is swift and with very limited number of modes (22 modes). Figure 3.14 plot the displacement field for both PGD and FEM method with the maximum and minimum error marked in Figure 3.12. In Figure 3.14b, PGD is able to obtained the phrase but not the magnitude. Case 4 worked cause it avoid the variation of two parameters, and present it in terms of only wavenumber k.

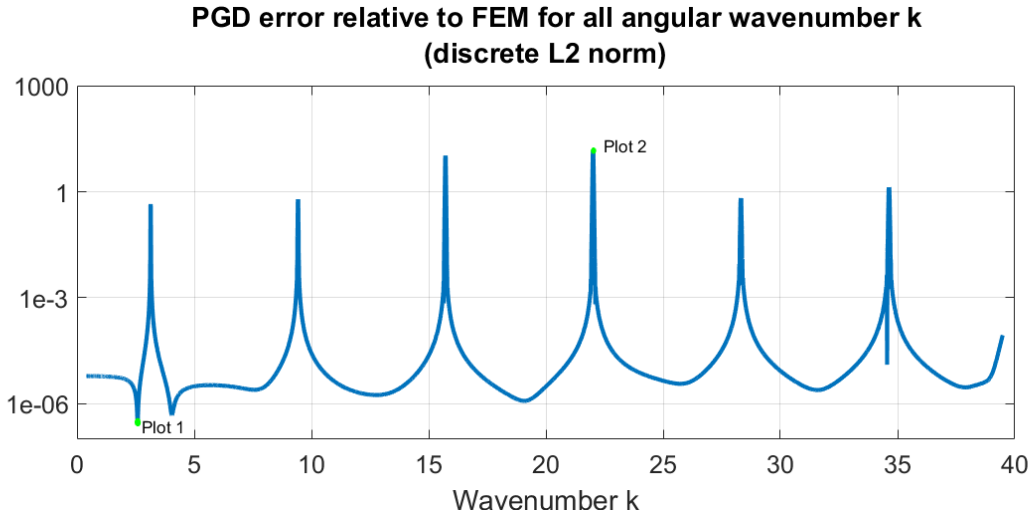

Figure 3.12: PGD errors for all angular wavenumber

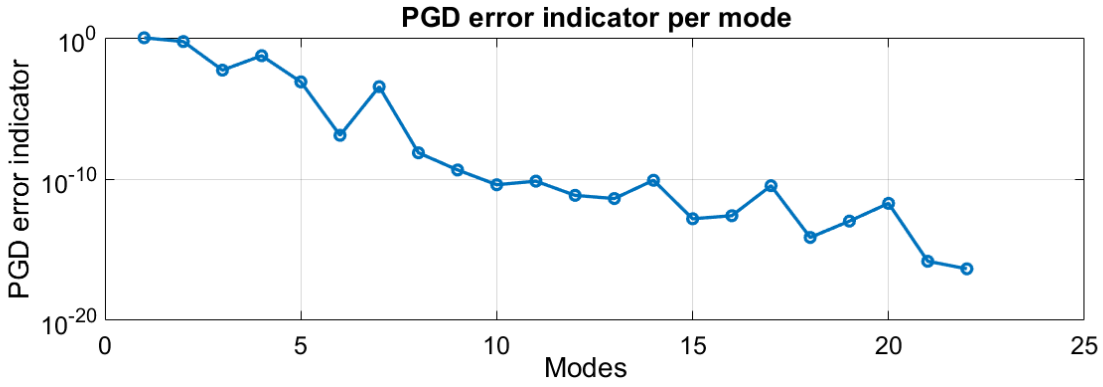

Figure 3.13: PGD error indicators for each mode

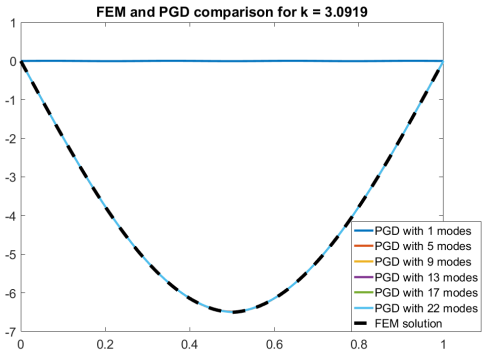

(a) Plot 1: The PGD and FEM displacement field for the minimum PGD error

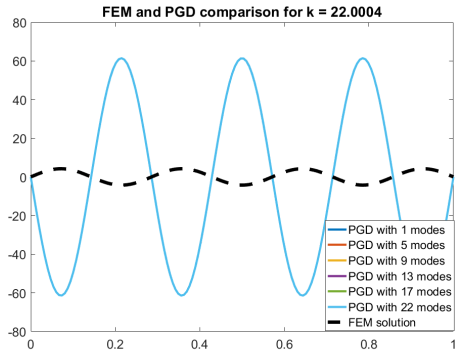

(b) Plot 2: The PGD and FEM displacement field for maximum PGD error

Figure 3.14: The displacement field by PGD and FEM solution

3.5 Case 5: Variable two layers of velocity

The last case is for obtaining the generalized solution for a spatial domain with two layers of velocity. The domain is separated into two sub-domain in the middle ($x = 0.5$). According to the analysis mentioned in Case 2, the velocity here is parameterized in terms of $\frac{1}{v^2}$. And the generalized solution for the displacement is obtained as $u(x, \frac{1}{v_1^2}, \frac{1}{v_2^2})$, where v_1 and v_2 present the velocity for sub-domain 1 and sub-domain 2 respectively. Similar as Case 3, the standard PGD cannot coverage for the velocity range used in Case 2. The maximum range of wavenumber for the method to be able to converge is $[1, 1.5]$, and the corresponding velocity is $v \in [1.0610, 1.5915]$. Furthermore, the tolerance for the last PGD terms is 10^{-14}, as the method is not about the converge within 500 modes for 10^{-16}.

The PGD error relative to FEM is given in Figure 3.15, the error is plotted as a surface and the magnitude of the error is around 10^{-6} except for one point (marked in yellow). Generally speaking, the error is acceptable in most part of Figure 3.15. There are jumps in error on the two edges marked by red dash box (when $v_1 = 1.0610$ and $v_2 = 1.0610$), which also exists in Figure 3.4. It proves the algorithm still have problem for velocity $v = 1.0610$. The maximum error is around 1, which is the point where $v_1 = v_2 = 1.0610$, when both two velocity domain have the same velocity that the PGD method have problem with. This can explain that the standard PGD method is not able to solve for large velocity range, as more troubled velocity will be introduced. Figure 3.16 presents the convergence of the standard PGD, the method convergent slowing to the tolerance (408 modes).

Furthermore, if using 10^{-10} as tolerance, the error is still acceptable as the similar L2 norm error as Figure 3.15 can also be obtained but with significantly less modes (136 modes).

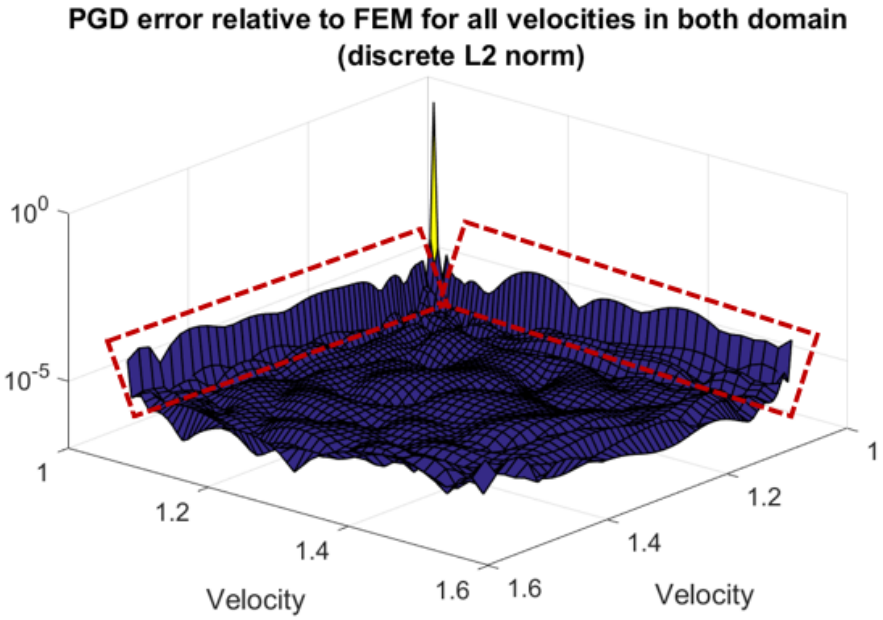

Figure 3.15: PGD errors for all velocities(in both domain 1 and domain 2)

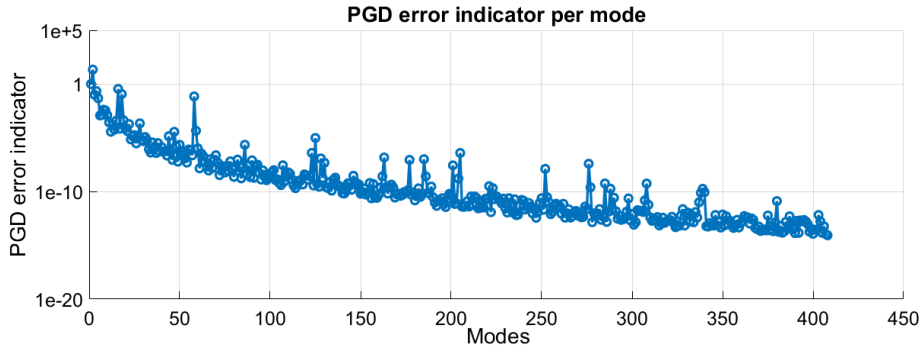

Figure 3.16: PGD error indicators for each mode

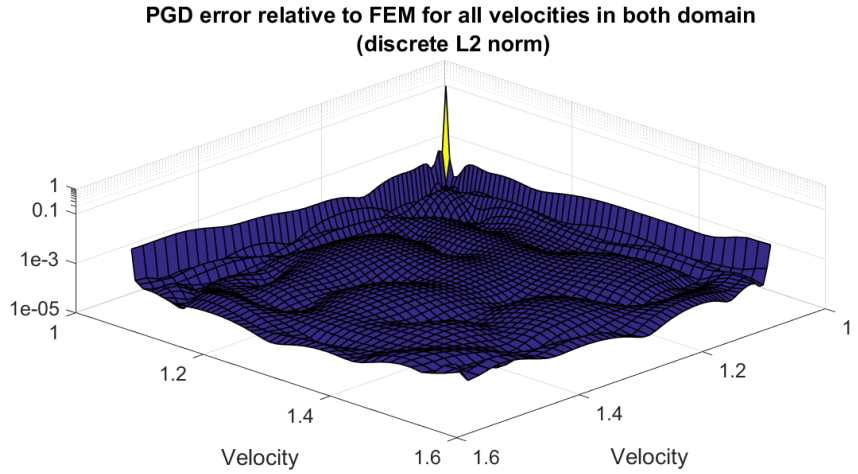

Figure 3.17: PGD errors for all velocities(in both domain 1 and domain 2)

4 Conclusion

The report presents the application of PGD to approximate the generalized solution of the Helmholtz equation. The generalization includes variability of the parameter frequency and velocity. Moreover, the velocity can be considered to have different values at different parts of the domain. Five numerical cases are presented to study different aspectS of the generalized solution.

First two cases analyze the influence on the PGD algorithm with different types of parameterization for frequency and velocity. For frequency, in terms of the number of modes, parametrize with $u(x, \omega)$ and $u(x, k)$ is much efficient than $u(x, k^2)$. In between $u(x, \omega)$ and $u(x, k)$, the former is more suitable for low frequency and both methods behavior similarly for high frequency, so the better way to parametrize frequency is using $u(x, \omega)$. In terms of velocity, the performance for different parametrization of velocity depends on the value of velocity (or say, the wavelength). For short waves, the inverse of the velocity parametrization ($u(x, 1/v)$ and $u(x, 1/v^2)$) have better performance while for long wave $u(x, v)$ gives more accuracy. However, $u(x, 1/v)$ is not recommended as it requires more modes than the rest two parametrization.

Case 3 formed the generalized solution $u(x, \omega, 1/v^2)$ considering both frequency and velocity, parametrized the way that is suggested from the previous cases. For limited range, the results are satisfactory as the error between PGD and FEM solution is around 10^{-7}. However, for large range of parameters, the method failed to converge and the error is not unacceptable. Two solution is offered, one is to parametrize the displacement field in terms of $u(x, k)$, as the wavenumber k includes the varying in both velocity and frequency and the other solution is to improve the PGD method, such as Petrov-Galerkin PGD (PG PGD). Case 4 use the parameterization for $u(x, k)$, the method is capable to converge for large range of wavenumber smoothly and with minimum number of modes, except for some specific wavenumber that the algorithm have trouble with.

The formalization for multiple layers of velocities are developed, but in Case 4 only two layers are test, the generalized solution is given in terms of $u(x, 1/v_1^2, 1/v_2^2)$. Under a controlled range, the method converged successfully and obtained acceptable solution. However, for larger range of the wavenumber the algorithm failed to converge. The reason is similar to case 3, as the range increase, the velocities in Case 2 which the PGD method have problem of solving might overlapped when two velocity dimensions are considered, and that surpass the limitation of the algorithm.

In brief, standard PGD method is capable of solving the generalized Helmholtz Equation. However, for both velocity and frequency, there are certain values of parameter that the algorithm cannot obtained the satisfiable solution. And this problem will escalate when two parameter domain is introduced (for example case 3 and 5) which cause algorithm failed to converge. To solving the problem, more research is required to apply a more reasonable boundary condition or improve the standard PGD method.

Bibliography

[1] A. Barbarulo, P. Ladevéze, H. Riou, L. Kovalevsky, Proper Generalized Decomposition applied to linear acoustic: A new tool for broad band calculation, J. Sound Vib. 333 (11) (2014) 2422-2431.

[2] U. Hetmaniuk, R. Tezaur, C. Farhat, Review and assessment of interpolatory model order reduction methods for frequency response structural dynamics and acoustics problems, Int. J. Numer. Methods Eng. 90 (13)(2012) 1636-1662.

[3] T. Lassila, A. Manzoni, G. Rozza, On the approximation of stability factors for general parametrized partial dierential equations with a two level affine decomposition, ESAIM-Math. Model. Numer. Anal. 46 (6) (2012) 1555-1576.

[4] Y. Chen, J. S. Hesthaven, Y. Maday, J. Rodrguez, X. Zhu, Certi

ed reduced basis method for electromagnetic scattering and radar cross section estimation, Comput. Methods Appl. Mech. Eng. 233-236 (2012) 92-108.

[5] M. Ganesh, J. S. Hesthaven, B. Stamm, A reduced basis method for electromagnetic scattering by multiple particles in three dimensions, J. Comput. Phys. 231 (23) (2012) 7756-7779.

[6] Kerschen G, Golinval JC, Vakasis AF, Bergman LA. The method of proper orthogonal decomposition for dynamical characterization and order reduction of mechanical systems: An overview. Nonlinear Dynamics , Springer 2005; 41:147–169.

[7] K. Karhunen, Uber lineare methoden in der wahrscheinlichkeitsrechnung, Ann. Acad. Sci. Fenn. 37 (1946) 1-79.

[8] M. Loéve, Probability Theory, 3rd Edition, Van Nostrand Princeton, 1963.

[9] G. Berkooz, P. Holmes, J. L. Lumley, The proper orthogonal decomposition in the analysis of turbulent ows, Annu. Rev. Fluid Mech. 25 (1) (1993) 539-575.

[10] Haasdok B, Ohlberger M, Rozza G. A reduced basis method for evolution schemes with parameter-dependent explicit operators. Electronic Transactions on Numerical Analysis 2008; 32:145–161.

[11] A. K. Noor, J. M. Peters, Reduced basis technique for nonlinear analysis of structures, AIAA J. 18 (4) (1980) 455-462.

[12] A. Ammar, B. Mokdad, F. Chinesta, R. Keunings, A new family of solvers for some classes of multidimensional partial dierential equations encountered in kinetic theory modelling of complex uids, J. Non- Newtonian Fluid Mech. 139 (2006) 153-176.

[13] A. Ammar, B. Mokdad, F. Chinesta, R. Keunings, A new family of solvers for some classes of multidimensional partial dierential equations encountered in kinetic theory modeling of complex uids. Part II: transient simulation using space-time separated representations, J. Non-Newtonian Fluid Mech. 144 (2007) 98-121.

[14] F. Chinesta, A. Ammar, E. Cueto, Proper generalized decomposition of multiscale models, Int. J. Numer. Methods Eng. 83 (8-9) (2010) 1114- 1132.

[15] F. Chinesta, A. Ammar, F. Lemarchand, P. Beauchene, F. Boust, Alleviating mesh constraints: Model reduction, parallel time integration and high resolution homogenization, Comput. Methods Appl. Mech. Eng. 197 (5) (2008) 400-413.

[16] D. Gonález, A. Ammar, F. Chinesta, E. Cueto, Recent advances on the use of separated representations, Int. J. Numer. Methods Eng. 81 (5) (2010) 637-659.

[17] A. Ammar, D. Ryckelynck, F. Chinesta, R. Keunings, On the reduction of kinetic theory models related to

nitely extensible dumbbells, J. Non-Newtonian Fluid Mech. 134 (1-3 SPEC. ISS.) (2006) 136-147.

[18] P. Ladevéze, J.-C. Passieux, D. Néron, The latin multiscale computational method and the proper generalized decomposition, Comput. Methods Appl. Mech. Eng. 199 (21-22) (2010) 1287-1296.

[19] A. Nouy, A generalized spectral decomposition technique to solve a class of linear stochastic partial dierential equations, Comput. Methods Appl. Mech. Eng. 196 (45-48) (2007) 4521-4537.

[20] A. Nouy, A priori model reduction through proper generalized decomposition for solving time-dependent partial dierential equations, Comput. Methods Appl. Mech. Eng. 199 (2010) 1603-1626.

[21] F. Chinesta, P. Ladeveze, E. Cueto, A short review on model order reduction based on proper generalized decomposition, Arch. Comput. Methods Eng. 18 (4) (2011) 395-404.

[22] G. Giorgiani, D. Modesto, S. Fernández-Méndez, A. Huerta, High-order continuous and discontinuous Galerkin methods for wave problems, Int.J. Numer. Methods Fluids 73 (10) (2013) 883-903.

[23] H. Bériot, G. Gabard, E. Perrey-Debain, Analysis of high-order

finite elements for convected wave propagation, Int. J. Numer. Methods Eng. 96 (11) (2013) 665-688.

[24] A. Ammar, F. Chinesta, P. Díez, A. Huerta, An error estimator for separated representations of highly multidimensional models, Comput. Methods Appl. Mech. Eng. 199 (2010) 1872-1880.

[25] Modesto D, Zlotnik S, Huerta A. Proper Generalized Decomposition for parameterized helmholtz problems in heterogeneous and unbounded domains: application to harbor agitation. Comput. Methods Appl. Mech. Eng. 2015; 295:127–149, doi:10.1016/j.cma.2015.03.026.

[26] Michel Goossens, Frank Mittelbach, and Alexander Samarin. *The LaTeX Companion*. Addison-Wesley, Reading, Massachusetts, 1993.

[27] Albert Einstein. *Zur Elektrodynamik bewegter Körper*. (German) [*On the electrodynamics of moving bodies*]. Annalen der Physik, 322(10):891–921, 1905.

[28] Knuth: Computers and Typesetting,`http://www-cs-faculty.stanford.edu/~uno/abcde.html`